Laser-induced heating in optical traps

Peterman, E.J.G.; Gittes, F.; Schmidt, C.

published in
Biophysical Journal
2003

DOI (link to publisher)
10.1016/S0006-3495(03)74946-7

document version
Publisher's PDF, also known as Version of record

Laser-Induced Heating in Optical Traps

Erwin J. G. Peterman,* Frederick Gittes,† and Christoph F. Schmidt*
*Division of Physics and Astronomy, Vrije Universiteit, Amsterdam, The Netherlands, and †Department of Physics, Washington State University, Pullman, Washington 99164-2814, USA

ABSTRACT In an optical tweezers experiment intense laser light is tightly focused to intensities of MW/cm^2 in order to apply forces to submicron particles or to measure mechanical properties of macromolecules. It is important to quantify potentially harmful or misleading heating effects due to the high light intensities in biophysical experiments. We present a model that incorporates the geometry of the experiment in a physically correct manner, including heat generation by light absorption in the neighborhood of the focus, balanced by outward heat flow, and heat sinking by the glass surfaces of the sample chamber. This is in contrast to the earlier simple models assuming heat generation in the trapped particle only. We find that in the most common experimental circumstances, using micron-sized polystyrene or silica beads, absorption of the laser light in the solvent around the trapped particle, not in the particle itself, is the most important contribution to heating. To validate our model we measured the spectrum of the Brownian motion of trapped beads in water and in glycerol as a function of the trapping laser intensity. Heating both increases the thermal motion of the bead and decreases the viscosity of the medium. We measured that the temperature in the focus increased by 34.2 $\pm$ 0.1 K/W with 1064-nm laser light for 2200-nm-diameter polystyrene beads in glycerol, 43.8 $\pm$ 2.2 K/W for 840-nm polystyrene beads in glycerol, 41.1 $\pm$ 0.7 K/W for 502-nm polystyrene beads in glycerol, and 7.7 $\pm$ 1.2 K/W for 500-nm silica beads and 8.1 $\pm$ 2.1 K/W for 444-nm silica beads in water. Furthermore, we observed that in glycerol the heating effect increased when the bead was trapped further away from the cover glass/glycerol interface as predicted by the model. We show that even though the heating effect in water is rather small it can have non-negligible effects on trap calibration in typical biophysical experimental circumstances and should be taken into consideration when laser powers of more than 100 mW are used.

INTRODUCTION

Over the last decade optical traps (optical tweezers) and related techniques have been used increasingly as a tool for microscopic manipulation in biology (Gittes and Schmidt, 1996; Mehta et al., 1999; Molloy and Padgett, 2002; Svoboda and Block, 1994) and other fields (Ashkin, 1997; MacKintosh and Schmidt, 1999). For example, the force generation by molecular motors (Finer et al., 1994; Svoboda et al., 1993) has been studied as well as the mechanical properties of biopolymers (Kellermayer et al., 1997; Smith et al., 1996; Tskhovrebova et al., 1997). In a typical optical trapping experiment a near-infrared laser beam is focused close to the diffraction limit using a high-power, high-numerical-aperture microscope objective lens (Ashkin, 1997). The laser beam exerts a force on micrometer-sized particles with a refractive index larger than that of the surrounding medium, such that there is an effective potential minimum near the focus. The focus therefore serves as a three-dimensional trap for the particle, and forces of tens of piconewtons can be readily exerted on micrometer-sized polystyrene or silica particles in an aqueous medium. In order to obtain these forces, laser powers of typically tens to hundreds of milliwatts are used, leading to focal intensities exceeding MW/cm^2 (for comparison the intensity of bright sunlight on the surface of the earth is on the order of 100 mW/cm^2). The potential of thermal and nonthermal damage caused by these high intensities to (biological) samples has been a matter of concern and investigation (Ashkin et al., 1987; Liu et al., 1995, 1996; Neuman et al., 1999). One way of reducing nonthermal photodamage to many biological materials is to use near-infrared lasers (such as Nd:YAG, Nd:YLF, diode- or Ti:Sapphire lasers) rather than visible lasers. Using a vitality assay measuring the rotation rate of trapped bacteria, it was recently shown that single-photon-induced processes involving the presence of oxygen are responsible for the remaining nonthermal photo damage by near-infrared laser light (Neuman et al., 1999). The temperature increase due to trapping a particle in water has been roughly estimated to be rather low, i.e., on the order of 1 K/W (Block, 1990). At an air-water interface, Wurlitzer et al. measured ~5 K/W heating in the focus (Wurlitzer et al., 2001). In trapped human sperm cells, hamster ovary cells, and liposomes the temperature increase was measured to be on the order of 10°C/W, 11.5°C/W, and 14.5°C/W respectively (Liu et al., 1995, 1996). These temperature changes were measured by observing phase transitions in lipid monolayers and bilayers respectively. The temperature increase was described by both groups with a simple model involving heat generation by absorption of light in the focus and subsequent heat dissipation to the bulk solution. A more elaborate model was presented by Schönle and Hell (1998) without accompanying experimental data. In their model heat generation by absorption and conduction in the whole light cone is taken into account. However, they do not obtain

Submitted November 7, 2001, and accepted for publication October 16, 2002.

Address reprint requests to Erwin J. G. Peterman, Division of Physics and Astronomy, Vrije Universiteit, De Boelelaan 1081 HV, Amsterdam, The Netherlands. Tel.: +31-20-4447987; Fax: +31-20-4447899; E-mail: erwinp@nat.vu.nl.

0006-3495/03/02/1308/09 $2.00

steady-state solutions, but rather focus on short-time effect with an eye on short-pulse applications.

Here we report a more direct method to observe temperature changes in a focused laser beam which is based on the analysis of the thermal motion of a trapped bead. Trapping a polystyrene or silica bead is commonly used in optical tweezers experiments. In addition, we will present a model that takes into account more accurately the entire spatial profile of the focused beam in a low numerical aperture (NA) approximation. By comparing data taken in water and glycerol, we show that light absorption by and dissipation in the solvent is the primary determinant of the temperature change, rather than heat absorbed by the trapped particle. The (cooling) effect of the sample cell wall is part of the model and is also demonstrated in the experiments. Presenting data for two cases of solvents with rather different heat conductivities demonstrates the applicability of the model. The model can be used for all other cases (with not too high absorption) as long as heat absorption and conductivity are known, and the results are largely independent of trapped particle properties, provided again that the absorption is not too high. Goals of the paper are to present a correct physical picture of heating in optical tweezers and to provide a practical model for experimenters to use to calculate potential heating effects in their particular situations.

MATERIALS AND METHODS

Optical trapping

The setup used for optical trapping is schematically represented in Fig. 1 and has been described in detail elsewhere (Allersma et al., 1998). In short, it consists of a custom-built inverted microscope, capable of trans-illumination differential interference contrast microscopy and optical trapping with near-infrared light from a diode-pumped Nd:YVO_4 laser (1064 nm, Topaz 106C, Spectra Physics, Mountain View, CA).

Sample chambers were made of a coverslip and a microscope slide, glued together with double-stick tape and mounted on a stage which can be moved manually and, over a shorter range, electronically with a dual-axis piezo-actuated stage (P-775.00, Physik Instrumente).

To visualize the beads, the sample was illuminated with the 546-nm line of an Hg arc lamp (100 W, Zeiss). The transmitted light was collected with an objective (Zeiss, NeoFluar 100×, oil immersion, NA 1.3) and imaged onto a camera (VT1000, Dage-MTI).

The laser-beam path consisted of two 3× beam expanders, a combination of a $\lambda/2$ plate and a Glan-laser polarizer (to adjust laser intensity), a 1:1 telescope (to position the trap focus in x-, y-, and z-directions), and beam steering mirrors. The laser beam was focused in the sample by the objective. The near-infrared and visible beam paths were separated using dichroic mirrors. Transmitted laser light was collected by the condenser (Zeiss, oil immersion, NA 1.4). Displacement of a bead trapped in the laser focus was measured in two dimensions, normal to the optical axis of the microscope (x, y) by imaging the back-focal plane of the condenser onto a quadrant photodiode (SPOT-9DMI, UDT Sensors) (Gittes and Schmidt, 1998a). The signals of this photodiode were amplified and anti-alias filtered using custom-built electronics, digitized with a PC board (AT-MIO16X, National Instruments or AD16/ChicoPlus, Innovative Integration), and further processed with custom software (LabView, National Instruments).

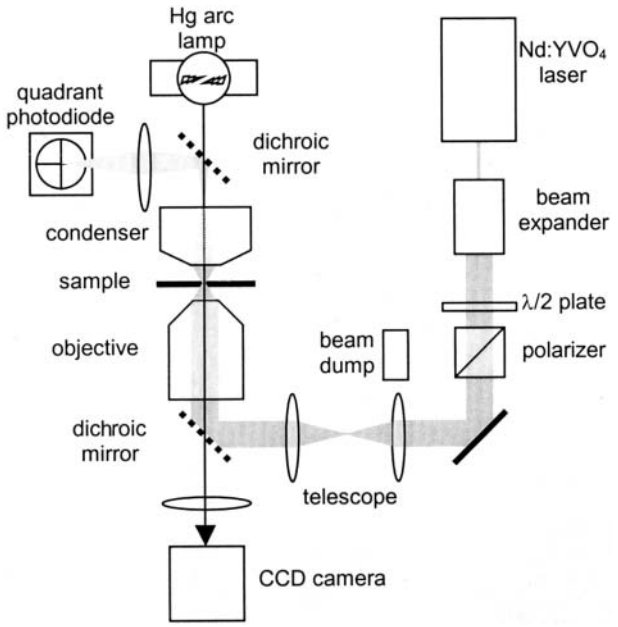

FIGURE 1 Schematic representation of the optical trap. The beam from a Nd:YVO_4 laser (1064 nm) is expanded with a beam expander and the power is regulated using the combination of a half-wave plate and a polarizer. After passing through a telescope, the first lens of which can be moved to reposition the trap, and being reflected by a dichroic mirror, the beam is focused into the sample with a microscope objective. This optical-trap beam path is represented by the gray line. The light which passes the sample is collected by a condenser, the back-focal plane of which is imaged onto a quadrant photodiode. This trap detection beam path is represented by the dashed gray line. For completeness, the ordinary image path is also shown (*black arrow*), which is formed by an Hg arc lamp which illuminates the sample via the condenser. The transmitted light is collected by the objective and imaged onto a tube camera. This (visible) beam is separated from the laser beam (1064 nm) by dichroic mirrors. For details, see text.

To exactly determine the laser intensity in the objective focus, the transmission of the objective was measured by replacing the condenser with an identical objective and measuring the transmitted light. We measured the transmission of this particular objective at 1064 nm as 62 ± 2%, in agreement with values published by others for the same brand and type of objective (Liu et al., 1995; Neuman et al., 1999; Svoboda and Block, 1994).

Optical absorption of water and glycerol

The optical absorption of glycerol and water at 1064 nm was determined by measuring the transmitted intensity of a laser beam passing through a cuvette filled with a variable path length of the respective liquid. The cuvette was made from an acrylic glass cylinder, oriented vertically, open on the top and closed with a cover glass at the bottom. Liquid was pumped in with a syringe connected to the side of the cylinder, close to the bottom. Another coverslip was placed inside the cylinder floating on top of the liquid layer, in order to obtain a flat meniscus. The water and glycerol where filtered through a 0.2-μm syringe filter and care was taken to avoid air bubbles. The height of the liquid column was measured with a precision ruler. Laser light (from a diode-pumped Nd:YVO_4; Topaz 106C, Spectra Physics, Mountain View, CA) was sent through the cuvette and the transmitted light intensity was measured with a laser power meter (Newport 1815-C with detector head 818T-10) as a function of the variable liquid path length in the cuvette as shown in Fig. 2. The extinction coefficients could be extracted from these data by fitting

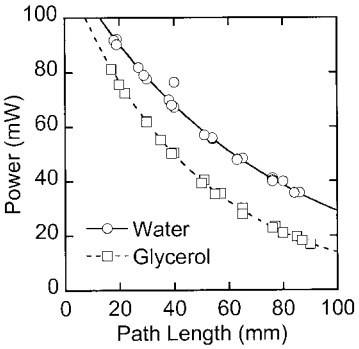

FIGURE 2 Transmitted laser power as a function of path length in water (*circles*) and glycerol (*squares*). The data are fitted (*solid* and *dotted lines* for water and glycerol, respectively) by the exponential function: $I(x) = I_0 \times e^{-\alpha x}$. The constant, α, was determined to be 14.2 m^{-1} for water and 21.4 m^{-1} for glycerol.

a single exponential function. The extinction coefficients were found to be 14.2 m^{-1} for water (similar to the ~12 m^{-1} obtained from the graph in Hale and Querry (1973) and 21.4 m^{-1} for glycerol.

Heating in the trap

Experiments were performed in a temperature controlled laboratory (294.6 ± 1 K). Samples consisted of highly diluted solutions of beads in glycerol or water. Care was taken to use anhydrous glycerol, in order to avoid a decrease of viscosity due to traces of water. Both polystyrene beads (with a diameter of 502 nm, Polybead, Polysciences; 834 nm and 2200 nm, both Seradyn) and silica beads (with a diameter of 444 nm, kind gift of the Colloid Synthesis Facility, Utrecht University, The Netherlands; and 500 nm, kind gift from E. Matijević, Clarkson University, NY) were used. Unless stated differently, single beads were trapped ~10 μm above the coverslip-liquid interface to avoid thermal and hydrodynamic surface effects.

The effect of heating in the focus of the trapping beam was measured in two ways. First, power spectra of the Brownian motion of a bead in the trap were measured as function of the laser power, and second, displacements of trapped beads were measured upon exertion of viscous drag (by moving the sample chamber using the piezo-actuated stage), also as a function of laser power.

RESULTS

The power spectra, $S(f)$, of the Brownian motion of a bead trapped in a laser focus can be approximated by a Lorentzian (Gittes and Schmidt, 1998a),

$$S(f) = \frac{S_0 \times f_0^2}{f_0^2 + f^2}, \quad S_0 \equiv \frac{4\gamma \times k_B \times T}{\kappa^2}, \quad f_0 \equiv \frac{\kappa}{2\pi \times \gamma}, \quad (1)$$

where S_0 is the zero-frequency intercept of the spectrum, $\gamma = 3\pi \times \eta \times d$ is the Stokes' drag of the bead with diameter d in a solvent with viscosity η, k_B is the Boltzmann constant, T is the absolute temperature, κ is the trap stiffness, and f_0 is the corner frequency of the spectrum. Some typical power spectra of a 502-nm-diameter polystyrene bead in glycerol are shown in Fig. 3. If the laser power only affected the trap stiffness κ (see Eq. 1), the corner frequency f_0 would increase with increasing power. For high frequencies, the f_0^2 term in the denominator of Eq. 1 becomes negligible, and the spectral density would become independent of trap stiffness and thus independent of laser power. If, on the other hand, the temperature, T, in the vicinity of the bead were to change with power, the spectral density would change also at high frequencies. Such an effect is evident in the data (Fig. 3) from the fact that the slanting parts of the spectra ($f > f_0$) do not overlap.

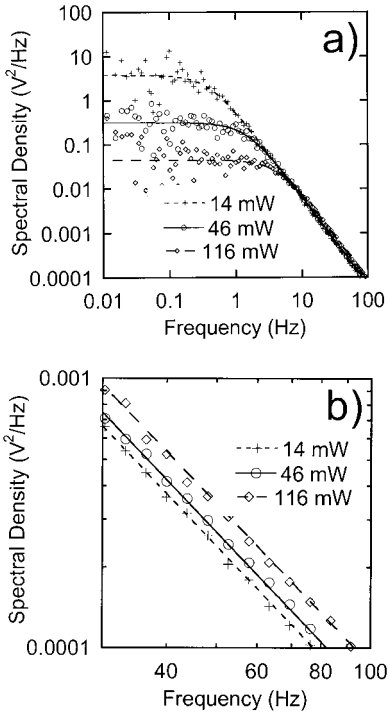

FIGURE 3 Power spectra of the Brownian motion of a trapped, 502-nm-diameter polystyrene bead in glycerol. The laser power was as indicated. The lines represent fits of Eq. 1 to the data. In (*a*) the whole spectra are shown; in (*b*) the high frequency regions of the spectra, where temperature effects are most clearly visible, are enlarged (see text).

In the following it will be shown, both experimentally and theoretically, that the observed power dependence of the spectra is due to heating in and around the focus as a result of absorption of the near-infrared laser light primarily by the solvent. Temperature influences the power spectra in two ways: (*i*) directly (the temperature factor in Eq. 1) and (*ii*) via the viscosity of the solvent, which is in general strongly dependent on temperature (Daubert and Danner, 1989; Weast, 1973). In order to quantify these effects, power spectra, like the ones in Fig. 3, were fitted by Eq. 1. Examples of such fits are shown in Fig. 3.

From Eq. 1, the laser–power dependence of the two fitted parameters (f_0 and $S_0 \times f_0^2$) can be expressed as

$$\frac{P}{f_0} \propto \eta(T_0 + B \times P) \quad (2)$$

and

$$\frac{1}{S_0 \times f_0^2} \propto \frac{\eta(T_0 + B \times P)}{(T_0 + B \times P)}, \quad (3)$$

where P is the laser power delivered to the sample, T_0 the temperature at zero laser power (294.55 K in these experiments), and B is the temperature increase in Kelvin-per-Watt (K/W) laser power near the focus. The temperature dependences of the viscosity (in Pa $\times$ s) of water (Weast, 1973) and glycerol (Daubert and Danner, 1989) are:

$$\eta_{\text{glycerol}}(T) = T^{31.734} \times e^{(-237.03+16739/T)}$$

$$\log(\eta_{\text{water}}(T)) = \frac{1.3272 \times (293.15 - T) - 0.001053 \times (T - 293.15)^2}{T - 168.15} - 2.999 \quad \text{for } T > 293.15 \text{ K}.$$

The power dependence of P/f_0 and $1/(S_0 \times f_0^2)$ for a polystyrene bead with diameter 502 nm in glycerol and a silica bead with diameter 444 nm in water are shown in Fig. 4. Also shown are fits of the data by Eqs. 2 and 3. The fit results for 502-nm (the experiments shown in Figs. 2–4), 840-nm, and 2200-nm polystyrene beads in glycerol and 444-nm (the experiments shown in Fig. 2) and 500-nm silica beads in water are listed in Table 1. These experiments indicate that in the case of glycerol the temperature increase is 41.1 $\pm$ 0.7 K/W laser light for the 502-nm beads, 43.8 $\pm$ 2.2 K/W for the 840-nm beads, and 34.2 $\pm$ 0.1 K/W for the 2200-nm beads. There is only a small effect coming from the size of the trapped bead. In water the temperature increase is substantially smaller than in glycerol, namely 7.7 $\pm$ 1.2 K/W for 500-nm beads and 8.1 $\pm$ 2.1 K/W for 444-nm beads. This is due to the lower absorption of 1064-nm light by water and the higher thermal conductivity of water (see below).

In Fig. 4 *E*, the temperature coefficient B for beads trapped at different distances from the glass–coverslip interface in glycerol is shown. This plot shows that the heating coefficient depends on the distance of the bead from the coverslip, which acts as a heat sink (see below). The closer the bead to the coverslip, the smaller the heating.

A value for the temperature coefficient B in glycerol was obtained in an independent way (for a distance of the bead from the coverslip of 10 μm). The displacement of a trapped

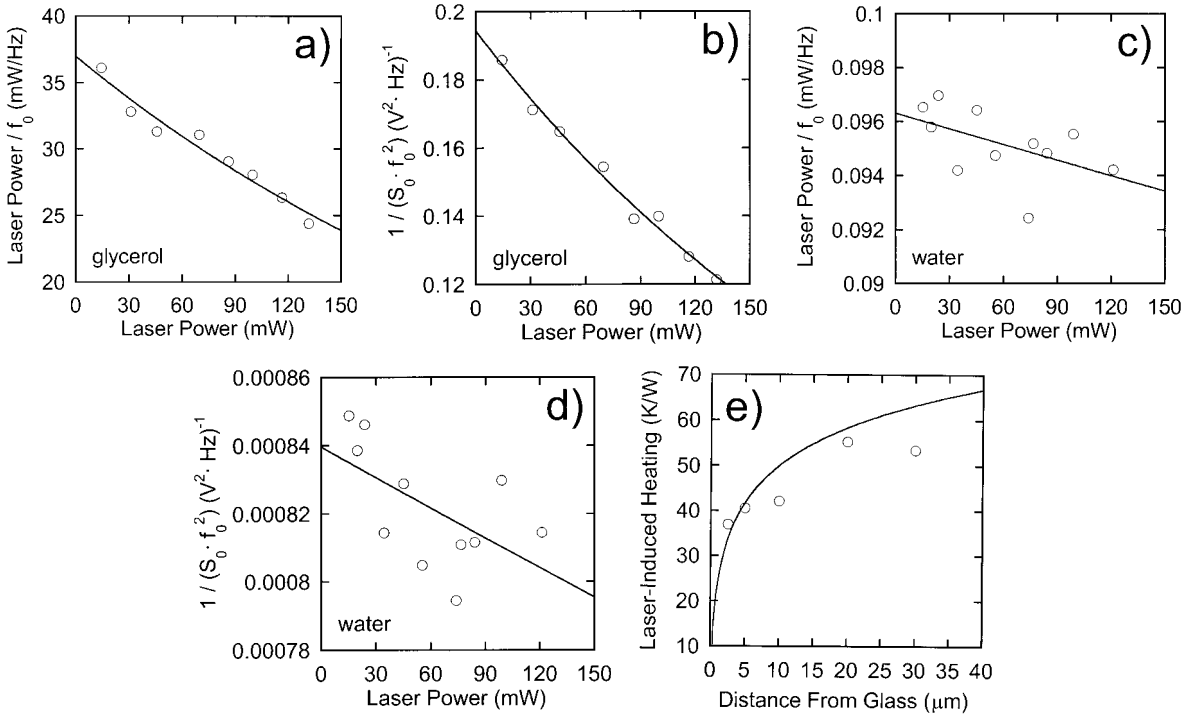

FIGURE 4 Laser-power dependence of the parameters obtained by fitting the power spectra of the Brownian motion of a trapped, 502-nm-diameter polystyrene bead in glycerol (*a*) and (*b*) and a 444-nm-diameter silica bead in water (*c*) and (*d*) at a distance of 10 μm from the glass solvent interface: *a* and *c* the laser power divided by the corner frequency (*line*, fit of data by Eq. 2); *b* and *d* the reciprocal of the product of the square of the corner frequency and the

TABLE 1 Summary of the experimentally determined values for the laser-induced heating. Shown are the results of fits to the power spectra of thermal motion of trapped beads (as shown in Fig. 4; the two values shown are obtained from the two perpendicular directions of motion of the bead in the plane normal to the trapping laser), and to the viscous drag experiments (Fig. 5)

				Laser-induced heating (K/W)			
Solvent	Bead material	Bead diameter (nm)	Distance from interface (μm)	From fit to P/f_0 (Eq. 2)	From fit to $f_0^2 \times S_0$ (Eq. 3)	From fit to $\Delta x \times P$ (Eq. 5)	(Weighted) average ± SE
Glycerol	Polystyrene	2200	10	–	34.2 ± 1.3		34.2 ± 0.1
				–	34.5 ± 3.3		
Glycerol	Polystyrene	840	10	47.2 ± 3.9	46.5 ± 2.2	39.2 ± 2.0	43.8 ± 2.2
				31.8 ± 5.1	47.3 ± 2.1		
Glycerol	Polystyrene	502	10	46.9 ± 10.6	40.6 ± 3.3		
				39.3 ± 2.1	41.0 ± 2.0	43.5 ± 1.0	42.2 ± 0.5
				47.0 ± 5.4	42.9 ± 2.7		
				38.8 ± 5.7	42.0 ± 0.9		
Glycerol	Polystyrene	502	5	–	39.3 ± 2.1		40.6 ± 1.7
				34.9 ± 4.4	42.8 ± 1.9		
Glycerol	Polystyrene	502	2.5	42.7 ± 4.1	39.0 ± 2.1		37.0 ± 1.8
				29.8 ± 4.8	35.2 ± 1.9		
Glycerol	Polystyrene	502	20	45.9 ± 8.8	57.6 ± 5.8		55.3 ± 1.5
				54.6 ± 3.6	56.5 ± 3.3		
Glycerol	Polystyrene	502	30	–	57.2 ± 3.1		53.4 ± 4.2
				53.4 ± 4.2	57.5 ± 2.7		
Water	Silica	500	10	9.2 ± 6.2	3.8 ± 6.3		7.7 ± 1.2
				9.5 ± 5.3	7.8 ± 5.2		
Water	Silica	444	10	8.5 ± 4.7	13.4 ± 6.2		8.1 ± 2.1
				2.5 ± 7.7	4.8 ± 7.6		

bead with respect to the center of the trap as a function of the laser power was measured while moving the sample stage (thus the surrounding glycerol) back and forth with constant speed. This displacement (Δx) is proportional to the force exerted on the bead and is equal to

$$\Delta x = \frac{F}{\kappa} = \frac{3\pi \times \eta \times d \times v}{\kappa}, \quad (4)$$

where v is the speed of the sample movement (in the present experiments 910 nm/s). A typical time trace of the displacement of a trapped polystyrene bead with a diameter of 502 nm is shown in Fig. 5 *A*. The sample chamber was moved back and forth with a constant speed of 910 nm/s at 0.1 Hz. The average displacement is determined by measuring the difference in position of the two peaks in a position histogram (Fig. 5 *B*) due to the alternating movement in opposing directions. The displacement is dependent on the laser power in two ways: *i*) the trap stiffness is proportional to the laser power and *ii*) the viscosity of the solvent depends on the laser power (via laser-induced heating):

$$\Delta x \times P \propto \eta(T_0 + B \times P). \quad (5)$$

Displacements (multiplied with the laser power) as a function of laser power are shown in Fig. 5 *C*. Also

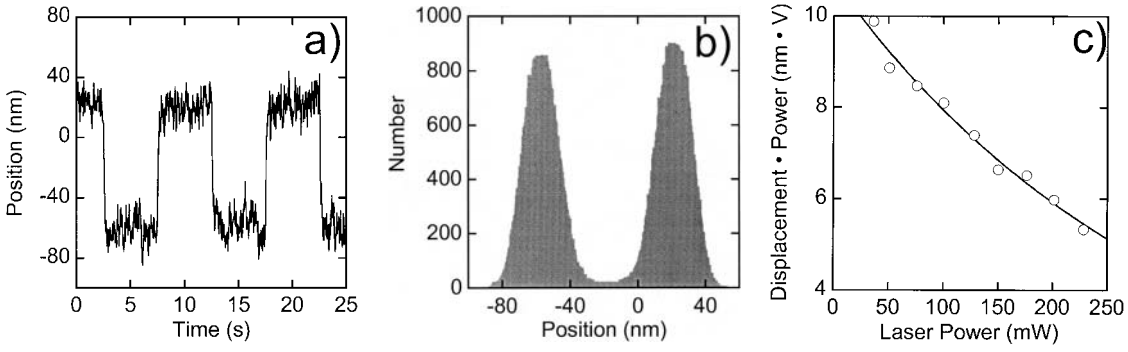

FIGURE 5 (*a*) Position time trace of a 502-nm-diameter polystyrene bead in glycerol when periodically moving the sample back and forth at 0.1 Hz with constant speed 910 nm/s. (*b*) Position histogram of the time trace in *a*. (*c*) Laser-power dependence of the product of laser power and displacement out of the laser trap as determined from histograms as in *b*. Circles represent the data, the line represents a fit of the data by Eq. 5.

shown is a fit of the data by Eq. 5. From this fit a temperature factor of 36.6 ± 2.0 K/W was obtained (see Table 1). For the 444-nm beads a temperature factor of 39.2 ± 2.2 K/W was measured. The values obtained for the laser-induced temperature increase obtained from the fluid-drag experiments are in agreement with those obtained from the power spectra (Table 1).

THEORETICAL MODEL

In this section we present a model for the temperature increase in the focus of a laser beam in a fluid. The experimental situation considered in the model is schematically shown in Fig. 6. We assume that the heating effect is primarily due to absorption of light by the fluid. Effects of the trapped particle are ignored at first. Later we will add a correction term which takes into account heat absorbed in the particle and will show that the effect of the bead size is relatively minor, as observed in the experiment. This justifies the above assumption.

The heat per volume, Q, generated per time by transmitting a plane wave of light with intensity, I, through a solvent, in the x-direction is given by

$$\frac{dQ}{dt} = -\frac{dI}{dx} = \alpha \times I, \tag{6}$$

where α is the extinction coefficient of the solvent, defined by $I(x) = I_0 \times e^{-\alpha x}$.

The heat generated by the absorption will dissipate. The dissipating heat flow $J(\vec{r})$ obeys the local differential equation

$$J(\vec{r}) = -C \times \nabla(\Delta T(\vec{r})), \tag{7}$$

where C is the thermal conductivity (for water, 0.60 W/(m × K); for glycerol, 0.28 W/(m × K); and for glass ~1.4 W/(m × K); Weast, 1973) and $\Delta T(\vec{r})$ is the temperature deviation from ambient temperature due to heating at position $\vec{r}$. In steady state the heat dissipated is equal to the heat generated: $\nabla J = \delta Q/\delta t$. Using Eqs. (6) and (7), this becomes:

$$\nabla^2(\Delta T(\vec{r})) = -\frac{\alpha}{C} \times I(\vec{r}). \tag{8}$$

This is general and does not hold only for a plane wave of light. To obtain $\Delta T(\vec{r})$, a model for the intensity profile of the laser is needed. Here a more accurate approximation of the intensity profile is considered than in a model published before (Liu et al., 1995). Suppose a laser of total power W_0 is brought to a focus at $r = 0$ (using spherical coordinates r, φ, and θ, with $\theta = 0$ along the incoming optical axis). To describe the beam intensity I, suppose that

$$I(\vec{r}) = W_0 \times \frac{f(\theta)}{r^2 + a^2} \tag{9}$$

(incoming for $\theta < \pi/2$, outgoing for $\theta > \pi/2$). At high NA, $f(\theta)$ could be quite a broad function of angle. At large distances, this incoming or outgoing intensity falls off as an inverse-square law,

$$I(\vec{r}) \approx P \times \frac{f(\theta)}{r^2}. \tag{10}$$

A total incoming intensity of P implies that $f(\theta)$ is normalized over incoming solid angle,

$$\int_{\theta<\pi/2} f(\theta)d\Omega = 1, \quad \int_{\text{all}\theta} f(\theta)d\Omega = 2, \tag{11}$$

where $d\Omega = \sin\theta\, d\theta\, d\varphi$. (The attenuation in Eq. 6 is assumed to be small, so that the outgoing power has been set equal to the incoming power.) To clarify Eq. 9, we derive the function $f(\theta)$ and the constant a for the case of a Gaussian beam, which is a low NA approximation for a focused laser. Manipulating well-known expressions (Siegman, 1986), one can write the far-field intensity distribution for a Gaussian beam in the form,

$$f(\theta) \propto e^{-\theta^2/\theta_0^2}, \tag{12}$$

where θ_0 is the equivalent angular radius of a uniformly illuminated aperture with the same total power. In terms of θ_0 one finds that the intensity of the Gaussian beam through the focus (along the $\theta = 0$ axis) has the form

$$I(\vec{r}) \propto \frac{1}{r^2 + (\lambda/2\pi\theta_0^2)^2} \tag{13}$$

which is of the form Eq. 9 with $a = \lambda/2\pi\theta_0^2$. The NA in this approximation is just $\theta_0 \approx \sin\theta_0$, so a plausible extrapolation to NA ≈ 1 gives $a = \lambda/2\pi$ in Eq. 9.

We are interested in solving Eq. 8 for the temperature in the focus, $T(0)$. The Green's function for Eq. 8 satisfies

$$\nabla^2 G(\vec{r},\vec{r}\,') = \delta^3(\vec{r} - \vec{r}\,'). \tag{14}$$

Here, $\delta(\vec{r})$ is the Dirac delta function. The Green's function with its argument $\vec{r}\,'$ set to zero and obeying

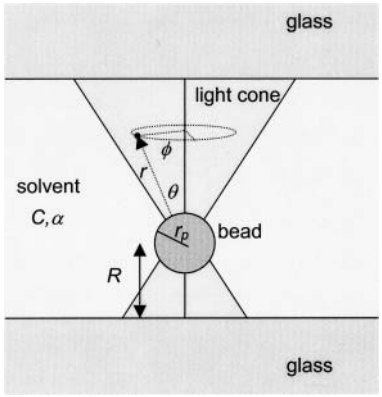

FIGURE 6 Schematic representation of the experimental situation considered in the model. For details, see text.

the boundary condition $G = 0$ at some large radial distance R, is

$$G(r) = -\frac{1}{4\pi}\left(\frac{1}{r} - \frac{1}{R}\right). \tag{15}$$

The $G = 0$ boundary condition might represent, for example, distant glass surfaces of higher heat conductivity (and lower attenuation). In terms of $G(r)$, the solution $\Delta T(r)$ of Eq. 8 at the origin is

$$\Delta T(0) = \int G(r)\left(-\frac{\alpha}{C} \times I(r)\right) dV \tag{16}$$

or, using Eqs. 13 and 15 and setting $\partial V = r^2\, dr\, d\Omega$,

$$\begin{aligned}\Delta T(0) &= \frac{\alpha \times P}{4\pi \times C} \times \int_{r<R} \frac{r^2 \times f(\theta)}{r^2 + a^2} \times \left[\frac{1}{r} - \frac{1}{R}\right] dr d\Omega \\ &= b \times P \times \int_0^R \frac{r^2}{r^2 + a^2} \times \left[\frac{1}{r} - \frac{1}{R}\right] dr, \quad b \equiv \frac{\alpha}{2\pi \times C}, \\ &\approx b \times P \times [\ln(R/a) - 1]\end{aligned} \tag{17}$$

where the integral is performed and the terms proportional to a/R are dropped. Then a is put equal to $\lambda/2\pi$ to get

$$\begin{aligned}\Delta T(0) = B \times P = b \times [\ln(2\pi \times R/\lambda) - 1] \times P, \\ b \equiv \frac{\alpha}{2\pi \times C}.\end{aligned} \tag{18}$$

The coefficient b has units of temperature per Watt (total) laser intensity and is equal to 3.8 K/W for water and 12.2 K/W for glycerol. Assuming the cutoff R is 10 μm (which is the distance of the bead from the cover glass in our experiments), the temperature increase (B) is 12 K/W for water and 38 K/W for glycerol (for $\lambda = 1064$ nm), close to the experimentally determined values. It is important to note that the experimentally found difference between glycerol and water is reproduced by the model, indicating that indeed the determining parameters for the heat generation are absorption of light, as governed by the extinction coefficients, α, and dissipation of the heat, as governed by the thermal conductivity, C. It should be noted that the dependence of the temperature difference on R is not very strong: if R was 100 μm, the temperature increase would be 21 K/W for water and 66 K/W for glycerol. Our experiments show that, indeed, the temperature increase is larger if the distance to the cover glass is larger. In general, in diffusion problems the shortest length scale dominates the effect, which is reflected in the logarithmic distance dependence. In reality the cutoff (i.e., the glass coverslip) is close only on one side. To obtain readily solvable equations, a symmetric cutoff R was assumed (as if the bead were in the center of a chamber, with varying thickness $2R$). In Fig. 4 E the data is compared to the distance dependence of Eq. 8. Within the error margins of the experiment this simplified model describes the data well without any fitting parameters.

In the preceding discussion we ignored the influence of the trapped particle. To obtain a more accurate description of the heating effect, a correction term can be added to Eq. 18 that incorporates the difference in absorption and thermal conductivity of the bead compared to the solvent. We represent these effects as an effective change in the coefficient b over the volume of the bead:

$$d(\Delta T(0)) = db \times P \times \frac{\ln\left[(r_p/a)^2 + 1\right]}{2}, \quad db \equiv d\left(\frac{\alpha}{2\pi \times C}\right), \tag{19}$$

where r_p is the radius of the trapped particle. For silica the absorption factor is on the order of 5×10^{-3} m^{-1} (Melles Griot catalog, 2001), the thermal conductivity 1.4 W/m K (Weast, 1973). For polystyrene we estimate the absorption factor to be 6 m^{-1} (Lytle et al., 1979), and the thermal conductivity is 0.12 W/m K (C.J.M. Lassence on http://www.electronics-cooling.com/html/2001_may_techdata.html). This means that the correction term to the heating coefficient (calculated with Eq. 19) due to a 500-nm silica bead in water is -2.2 K/W (i.e., 11–19% of that calculated with Eq. 18, assuming an R cutoff of 10 μm). For the polystyrene beads in glycerol the correction term is from -7.9 K/W (i.e., 21% of the uncorrected value for 1094-nm beads and -2.6 K/W (i.e., 7% of the uncorrected value) for the 502-nm beads. This shows that the effect of the trapped particle is relatively small. In our calculations it produces less of an effect than the choice of the R cutoff. Note that the calculation predicts that the heating in the vicinity of small (502-nm-diameter) polystyrene particles is larger than that around the larger (2200-nm) ones, and likewise for silica, inasmuch as absorption in the particles is weaker than in water or glycerol. Qualitatively, this is observed in the experiments.

Our experiments on fixed, trapped beads gave the same results as the drag experiments (in which the bead was held in place and the solvent was moved) suggesting that the heat equilibration is faster than the movement in these experiments. To estimate time scales for the equilibration time for any given temperature distribution, we need not only C (with units J/s $\times$ m $\times$ K) but also the heat capacity per volume c_V (for water 4.2×10^6 J/m$^3 \times$ K, for glycerol 3.0×10^6 J/m$^3 \times$ K). On dimensional grounds, the equilibration time to a given distance r must be on the order of $r^2 \times c_V/C$. Thus, for both water and glycerol, temperature equilibration out to 10 μm takes roughly 1 ms. The time-dependent heating model by Schönle and Hell (1998) does not apply to our situation, because they assume an infinite sample size, which causes the infinite equilibration times they report. Temperature kinetics should thus not be relevant even if the solvent is moved fairly quickly. In our drag experiments the sample

is moved with a speed of 910 nm/s, slow enough to allow temperature equilibration.

DISCUSSION

We have measured local solvent heating produced by a strongly focused 1064-nm continuous-wave laser beam used as optical tweezers in water and glycerol and have derived a simple model that captures the most important features of this process. In the experiments we obtained the laser-induced temperature increase from the analysis of the power dependence of the thermal motion of trapped beads (Table 1). A theoretical model that takes into account heat generation by absorption of light by the solvent in the whole beam path and dissipation of the heat into the bulk solvent reproduced both the absolute temperature increases for water and glycerol and the difference between the two solvents.

This value for the laser-induced heating is comparable to the values measured before (5 K/W, Wurlitzer et al., 2001; ~10–15 K/W; Liu et al., 1995, 1996). We think that our measurements are likely to be more accurate since well-defined solid particles (polystyrene, silica) were trapped, in contrast to some of the previous experiments where vesicles and cells were used. We have shown both experimentally and in our model that the effect of the trapped (polystyrene, silica) particles is only minor; the main contribution to the heating is light absorption by the surrounding solvent. The distance from the glass-solvent interface, however, has a substantial effect on the heating. We have shown that the heating increases substantially when the bead is trapped further away from the interface.

It remains to be discussed for which kind of experiments these results are relevant. Most optical trapping experiments use water (or watery solutions) as solvent and laser powers on the order of 100 mW (at 1064 nm). This leads to a temperature increase of only ~0.8 K in the focus, which, depending on the solvent, may change the viscosity more dramatically. In many cases the Lorentzian fit to a power spectrum of a trapped bead is used for the calibration of the trap and detector response (Gittes and Schmidt, 1998b). If the heating effect is not taken into consideration using this calibration method, the trap stiffness—which is proportional to the estimated viscosity (η) times the measured corner frequency (f_0)—is overestimated 2% (10%) when a laser power of 100 mW (500 mW) is used. Here we assume a temperature increase of 8 K/W and a base temperature of 294.55 K. The detector response (in m/V) is proportional to the temperature (T) divided by the viscosity (η) and the zero-frequency intercept of the power spectrum ($S_0 f_0^2$) and is in the same circumstances underestimated 2% and (11%). Consequently, heating effects due to laser-light absorption by the solvent in optical trapping experiments even in watery solution have a small but measurable effect, and should be taken into consideration, especially when laser powers higher than ~100 mW are used.

We thank Winfield Hill, Rowland Institute for Science, Cambridge, Massachusetts, for help with the electronics; Wolfgang Möhler for his contributions to the initial stage of the experiments; and the Colloids Synthesis Facility, Utrecht University, The Netherlands, and E. Matijević, Clarkson University, New York, for the supply of silica particles.

This research was supported by the Foundation for Fundamental Research on Matter (FOM). E.P. is supported by a Postdocs Universitaire Loopbaan Stimulerings Programma (PULS)-fellowship from the Research Council for Earth and Life Sciences (ALW) with financial aid from the Dutch Organization for Scientific Research (NWO).

REFERENCES

Allersma, M. W., F. Gittes, M. J. deCastro, R. J. Stewart, and C. F. Schmidt. 1998. Two-dimensional tracking of NCD motility by back focal plane interferometry. *Biophys. J.* 74:1074–1085.

Ashkin, A. 1997. Optical trapping and manipulation of neutral particles using lasers. *Proc. Natl. Acad. Sci. USA.* 94:4853–4860.

Ashkin, A., J. M. Dziedzic, and T. Yamane. 1987. Optical trapping and manipulation of single cells using infrared laser beams. *Nature.* 330: 769–771.

Block, S. M. 1990. Optical tweezers: a new tool for biophysics. *In* Noninvasive Techniques in Cell Biology. S. Grinstein, K. Foskett, editors. Wiley-Liss, New York, New York. 375–401.

Daubert, T. E., and R. P. Danner. 1989. Physical and Thermodynamic Properties of Pure Chemicals: Data Compilation. Hemisphere Pub. Corp., New York, New York.

Finer, J. T., R. M. Simmons, and J. A. Spudich. 1994. Single Myosin molecule mechanics—piconewton forces and nanometer steps. *Nature.* 368:113–119.

Gittes, F., and C. F. Schmidt. 1996. Microscopic approaches to dynamics and structure of biological motors. *Curr. Opin. Solid State Mat. Sci.* 1:412–424.

Gittes, F., and C. F. Schmidt. 1998a. Signals and noise in micromechanical measurements. *Methods Cell Biol.* 55:129–156.

Gittes, F., and C. F. Schmidt. 1998b. Thermal noise limitations on micromechanical experiments. *Eur. Biophys. J. Biophys. Lett.* 27: 75–81.

Hale, G. M., and M. R. Querry. 1973. Optical constants of water in the 200-nm to 200-μm wavelength region. *Appl. Optics.* 12:555–563.

Kellermayer, M. S. Z., S. B. Smith, H. L. Granzier, and C. Bustamante. 1997. Folding-unfolding transitions in single titin molecules characterized with laser tweezers. *Science.* 276:1112–1116.

Liu, Y., D. K. Cheng, G. J. Sonek, M. W. Berns, C. F. Chapman, and B. J. Tromberg. 1995. Evidence for localized cell heating induced by infrared optical tweezers. *Biophys. J.* 68:2137–2144.

Liu, Y., G. J. Sonek, M. W. Berns, and B. J. Tromberg. 1996. Physiological monitoring of optically trapped cells: assessing the effects of confinement by 1064-nm laser tweezers using microfluorometry. *Biophys. J.* 71:2158–2167.

Lytle, J. D., G. W. Wilkerson, and J. G. Jaramillo. 1979. Wideband optical transmission properties of seven thermoplastics. *Appl. Optics.* 18: 1842–1846.

MacKintosh, F. C., and C. F. Schmidt. 1999. Microrheology. *Curr. Opin. Colloid Interface Sci.* 4:300–307.

Mehta, A. D., M. Rief, J. A. Spudich, D. A. Smith, and R. M. Simmons. 1999. Single-molecule biomechanics with optical methods. *Science.* 283:1689–1695.

Molloy, J. E., and M. J. Padgett. 2002. Lights, action: optical tweezers. *Contemp. Phys.* 43:241–258.

Neuman, K. C., E. H. Chadd, G. F. Liou, K. Bergman, and S. M. Block. 1999. Characterization of photodamage to *Escherichia coli* in optical traps. *Biophys. J.* 77:2856–2863.

Schönle, A., and S. W. Hell. 1998. Heating by absorption in the focus of an objective lens. *Optics Lett.* 23:325–327.

Siegman, A. E. 1986. Lasers. University Science Books, Mill Valley, California.

Smith, S. B., Y. J. Cui, and C. Bustamante. 1996. Overstretching B-DNA: the elastic response of individual double-stranded and single-stranded DNA molecules. *Science.* 271:795–799.

Svoboda, K., and S. M. Block. 1994. Biological applications of optical forces. *Annu. Rev. Biophys. Biomolec. Struct.* 23:247–285.

Svoboda, K., C. F. Schmidt, B. J. Schnapp, and S. M. Block. 1993. Direct observation of kinesin stepping by optical trapping interferometry. *Nature.* 365:721–727.

Tskhovrebova, L., J. Trinick, J. A. Sleep, and R. M. Simmons. 1997. Elasticity and unfolding of single molecules of the giant muscle protein titin. *Nature.* 387:308–312.

Weast, R. C., editor. 1973. CRC Handbook of Chemistry and Physics, 53rd ed. CRC Press, Boca Raton, Florida.

Wurlitzer, S., C. Lautz, M. Liley, C. Duschl, and T. M. Fischer. 2001. Micromanipulation of Langmuir-monolayers with optical tweezers. *J. Phys. Chem. B.* 105:182–187.